Testing Characteristics of Grid Forming Converters Part III: Inertial Behaviour

A. Dyśko, A. Egea, Q. Hong, A. Khan
Department of Electronic and Electrical Engineering
University of Strathclyde
Glasgow, United Kingdom
a.dysko@strath.ac.uk

P. Ernst, R. Singer
Power Electronics, Grids and Smart Systems
Fraunhofer ISE
Freiburg i. B., Germany
roland.singer@ise.fraunhofer.de

A. Roscoe
Siemens-Gamesa Renewable Energy
Glasgow, United Kingdom
andrew.roscoe@siemensgamesa.com

***Abstract*— On the path towards an energy system powered entirely by Renewable Energy Sources (RES), power electronic converters will have to take over more and more functionalities from synchronous generators to ensure a stable and secure operation of the power grid. Moreover, it is widely recognised that the use of Grid Forming Converters (GFC) is necessary to fully meet these requirements. Over the last years, different concepts have been developed to achieve grid forming characteristics of static power converters. The next essential step is to agree on an exact definition and specification of GFC electrical behaviour as well as to define a suitable conformity assessment procedure. For this purpose, standardised testing guidelines for GFC are needed to assess those functionalities, which are relevant for dynamic grid stability. As a British-German joint work of the two research projects Battery-VSM and VerbundnetzStabil, the first draft of such guidelines is being currently developed.**

One of the necessary characteristics which makes converter a GFC is its ability to provide inertial response during the dynamic frequency changes in the system. This paper focuses on how to demonstrate and quantify an inertia-equivalent behaviour of a GFC. The response to a transient system event is quantified in terms of a damping factor *D* as well as an equivalent inertia constant *H*. A few alternative methods are proposed for empirical estimation of those parameters accompanied by selected laboratory test results and practical considerations.

Keywords—grid forming converter, virtual synchronous machine, virtual inertia, testing guideline, conformity assessment, voltage source properties, power quality, asymmetries, unbalance, harmonics, impedance spectroscopy, current limitation. overload, grid faults

I. INTRODUCTION

With the increasing penetration of Renewable Energy Sources (RES) in electricity generation, more and more energy is provided using power electronic converters. Furthermore, we are moving towards a future where RES together with battery storage can potentially supply all, or close to all, of the system demand in many countries, replacing Synchronous Generators (SG) used in conventional power plants. [1]

Nowadays, the full scope of ancillary services is typically provided by large synchronous machines. RES on the other hand are typically installed in such a way, that they act as sinusoidal current sources at fundamental frequency with limited functionalities. These sources are called grid following converters, controlling the current they feed into the grid. However, in order to sustain system stability, RES and storage systems will have to take over more system functionalities. This can be achieved by converters operating as voltage sources, which are called Grid Forming Converters (GFC). A categorization of inverter behaviour at fundamental frequency is given in Table I shown on the next page.

Over the last years, different control strategies have been developed claiming to be grid forming. A review and comparison of GFC control strategies is given in [2]. One of today's challenges is to reach a general consensus on the behaviour of GFC, and its verification. A solution to those two aspects is necessary for system operators, manufacturers, and energy providers so that they can define the specifications of their products for market integration, and to ensure interoperability between different products.

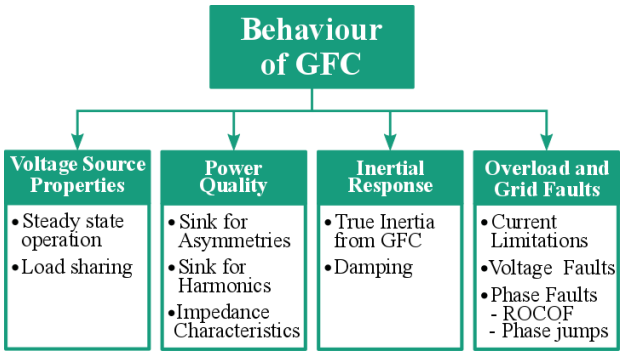

Fig. 1. Overview: Behaviour of Grid Forming Converters

The desirable behaviour of GFC has been discussed in recent studies, such as [3], [4], [5], [6] and [7]. An overview of the main issues which need to be considered is given in Fig. 1. The next step towards GFC certification is to line out the required specifications and to formulate a suitable conformity assessment procedure. First efforts on formulating directives for GFC have been made in [8] and [9]. As a British-German joint work of the two research projects Battery-VSM and VerbundnetzStabil, a first draft of a standardizing testing guideline for GFC is currently being developed. It defines detailed test setups, calculation of relevant device parameters as well as evaluation criteria.

Due to the complexity of the topic and the numerous aspects that need to be taken into account, the session entitled "Testing Grid Forming Converters" consists of four contributions:

1. Specification of GFC and Definition of GFC Behaviour,
2. Voltage Source Properties and Contribution to Power Quality,
3. Inertial Response,
4. Overload Behaviour and Response to Grid Faults.

Table I. Inverter Behaviour at Fundamental Grid Frequency

	Voltage controlled		Current controlled	
	Grid leading	Grid forming	Grid following	Grid supporting
Source type	Fixed voltage source	Controlled voltage source	Fix current source	Controlled current source
Control type	Provides fixed V & f (ref.)	Provides V & f (ref.), f(P), V(Q)	Follows P & Q (ref.)	Adjusts P & Q (ref.), P(f), Q(V)

This paper specifically focuses on the aspects of grid forming behaviour related to inertial response. The inertia and damping behaviour of a generator is first defined (Section II), followed by a short review of modelling approaches to describe such behaviour (Section III). Further on, a few alternative methods are proposed for empirical validation of the inertia parameters (Section IV), and a discussion on the practical consideration of implementing those methods in practice (Section V).

II. Inertial Response

The key requirements for GFCs in terms of voltage source behaviour, power rating and required energy storage to achieve the desired inertial response have been outlined in Part I of this series. However, a few fundamental definitions and relationships are also included here for reader's convenience.

According to GB operator National Grid's ESO most recent specification [10], inertia power is defined as "the (start of an) instantaneous short-term transfer of active power from the facility to or from the system following a system frequency change as a result of an instantaneous change in generation or demand on the system. This should occur without the need for any change in the internal voltage source of the facility." As mentioned before, "instantaneous" is meant to be a response within 5 ms.

Furthermore, the following equations are given:

$$Inertia = H \cdot S_{rating} \tag{1}$$

$$H = \frac{|\Delta P| \cdot f_0}{2 \cdot S_{rating} \cdot |RoCoF|} \tag{2}$$

with H being the inertia constant similar to a synchronous machine, S_{rating} being the rated apparent power of the GFC, f_0 being the system frequency before a frequency event, and ΔP being the active power increment as a result of a frequency event with a given constant *RoCoF*.

Regarding the damping, the UK's Grid Code draft [11] states that the damping active power is "the active power naturally supplied by a grid forming plant as a result of oscillations in the total system. More specifically, damping active power is the result of an oscillation between the voltage at the terminals of a grid forming unit and the voltage of the internal voltage source of the grid forming unit".

As inertia is most commonly characterised by the swing equation of a synchronous machine, it is generally considered beneficial that the GFC's inertial behaviour should also be parametrised in the same way, namely by inertia constant H and damping factor D. This way, the GFCs inertial behaviour could be conveniently adapted to existing grids [12] as the meaning and significance of those parameters is well understood both in theory and operational practice.

As for all characteristics of GFCs, inertia power, damping power and phase jump power can only be provided up to the current limitation of the converter. In [12], it is suggested to keep a current headroom in order to being able to provide inertia power even when operating stationary at nominal power.

III. Modelling of GFC Dynamic Behaviour

Several implementations of converter controllers for grid forming converters have been suggested in the literature [13]. In general, all of the most promising implementations mimic the behaviour of a synchronous generator in different level of detail. The common element of those implementations is that they have an active power synchronizing loop inspired in the swing equation. Fig. 2 shows the general representation of the synchronous machine swing equation.

A family of grid forming converter controllers are based on standard current control with an outer loop to mimic the behaviour of a synchronous machines [14]. This outer loop provides the current references and angle to the converter control. Another family of grid forming converters are based on the direct implementation of the swing equation and a voltage controller, similar to the synchronous machine [15]. Direct swing equation-based controllers have the ability to provide a faster response but the fault ride through in case of a fault might be challenging as no current control structure exists.

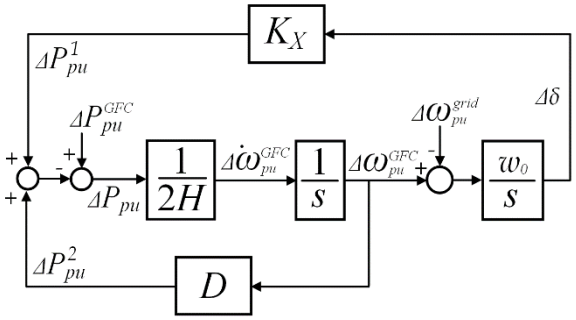

Fig. 2. Second order synchronous machine model assumed for represent GFC behaviour

IV. Empirical Estimation of Inertia and Damping Parameters

A. Time Domain Based Method

One possibility to estimate the inertia and the damping parameters is to analyse the time domain behaviour of the GFC. This method is based on a comparison between the GFC behaviour with a reference model in order to approximate the inertial response parameters.

The first step is to define an appropriate reference model. As the inertial response of the GFC should be similar to the synchronous machine, it is reasonable to use a simplified physical model of the SM. Since the dominant behaviour in a synchronous machine is defined by the swing equation, this approach uses the 2nd order differential equation represented by block diagram in Fig. 2.

With the assumptions:

$$\Delta\omega_{PU}^{grid} = 0 \tag{3}$$

$$\Delta\delta = \delta^{GFC} - \delta^{grid} \tag{4}$$

$$\frac{d\delta^{GFC}}{dt}\frac{1}{\omega_0} = \Delta\omega_{PU}^{GFC} \tag{5}$$

and the model in Fig.2, the state-space model can be written as shown in equations (6) and (7).

$$\begin{pmatrix}\Delta\omega_{PU}^{GFC} \\ \dot{\Delta\omega}_{PU}^{GFC}\end{pmatrix} = \begin{pmatrix}0 & 1 \\ -\frac{K_x}{2H} & -D\end{pmatrix}\begin{pmatrix}\delta^{GFC} \\ \Delta\omega_{PU}^{GFC}\end{pmatrix} + \begin{pmatrix}0 & 0 \\ \frac{1}{2H} & -\frac{K_x}{2H}\end{pmatrix}\begin{pmatrix}\Delta P_{PU}^{GFC} \\ \delta^{grid}\end{pmatrix} \tag{6}$$

$$\Delta P_{PU} = \begin{pmatrix}K_x & 0\end{pmatrix}\begin{pmatrix}\delta^{GFC} \\ \Delta\omega_{PU}^{GFC}\end{pmatrix} + \begin{pmatrix}0 & -K_x\end{pmatrix}\begin{pmatrix}\Delta P_{PU}^{GFC} \\ \delta^{grid}\end{pmatrix} \tag{7}$$

As can be seen, the reference system has two state variables, δ^{GFC} and $\Delta\omega_{PU}^{GFC}$, and two inputs, ΔP_{PU}^{GFC} and δ^{grid}. For the characterisation purposes the GFC must be perturbed by one of the inputs. The first option is applying a step function by changing the reference point ΔP_{GFC} of the GFC. However, in practice this would not be feasible as in a commercial converter the power reference is not likely to be applied to the inertia loop directly. Therefore, a change of the grid phase angle is a much more reliable choice for disturbance signal. After the reference model in time domain as well as the GFC trigger signal are defined, the model parameters can be approximated using a step response, denoted as $h_{GFC}(t)$.

$$minimise\left\{\sum_{t=t_{phase\ step}}^{t=t_{end}} |h_{ref}(t, H, D, K_X) - h_{GFC}(t)|\right\} \tag{8}$$

The parameters to optimise are the inertia constant, H the damping factor D and the maximum transmission power K_X. In order get better results, the parameter space can be reduced by calculating K_X, as the used impedances are known.

To validate the accuracy of the time domain model approach, several simulations with different inertial constants and phase jumps are carried out. The simulations are done with a detailed GFC model, including a VSM with a underlying voltage control combined with a model of the hardware. The results can be seen in Fig. 3. The blue curve is the response of the GFC model, the orange curve the reference model with the approximated parameters.

In Table II the approximated inertia and damping parameters are shown (in the same order as in the simulations). The total error is in case of the inertia constant H between 10.0% and 16.7%, whereas the damping error variates between 11.1% and 14.2%, so this can be seen, in both cases, as reasonably accurate. In order to reduce the influence of measurement noise (and/or other side effects), the test can be performed with a few different angle steps.

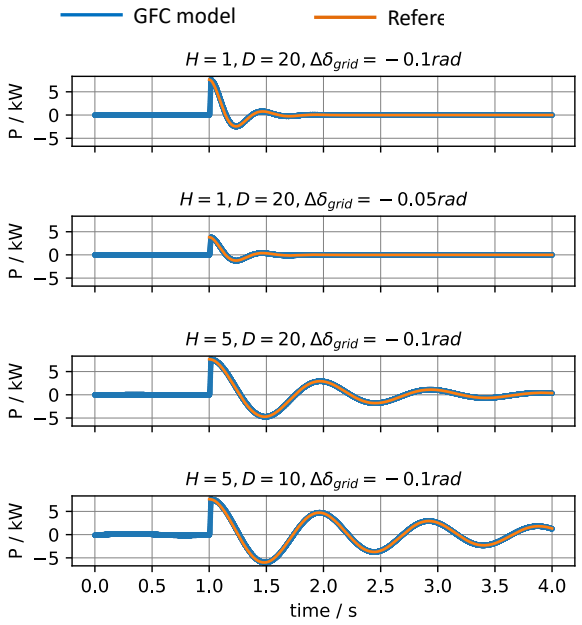

Fig. 3. Response of the GFC to phase jumps with different inertial settings

Table II. Approximated inertia constant of Fig.3

Case	H [s]			D [pu]		
	Actual	Approx.	Error	Actual	Approx.	Error
1	1	1.167	16.7%	20	22.748	13.7%
2	1	1.17	17.0%	20	22.834	14.2%
3	5	5.59	11.8%	20	22.216	11.1%
4	5	5.5	10.0%	10	11.129	11.3%

B. Frequently Domain Based Method

In control theory, a typical way of characterising any dynamic linear system is through transfer functions and associated Bode or Nyquist plots. Those can be very useful for visually assessing various dynamic characteristics of the generator which otherwise can be difficult to separate, such as droop, inertia and damping. In the paper [16] an innovative method termed Network Frequency Perturbation (NFP) was introduced where a Bode type characteristic of an inverter was obtained by modulating the voltage source frequency according to equation (9).

$$f = f_0 + \Delta f \cos(2\pi f_{NFPmod}) \tag{9}$$

Where:
f_0 = 50 Hz
Δf = 0.5 Hz (modulation amplitude - 1% of 50 Hz)
f_{NFPmod} – frequency of the modulation in Hz.

The test is repeated at changing values of modulation frequency and the power response ΔP_{pu} is captured each time, in terms of amplitude and phase of the resulting steady-state power modulation. The response characteristic is defined as R, a ratio of the per-unit power response (output) to the per-unit value of frequency perturbation (input), as shown in (10).

$$R = \frac{\Delta P_{PU}}{\left(\frac{\Delta f}{f_0}\right)} \tag{10}$$

Using the simplified synchronous generator dynamic model shown in Fig. 2, implemented in Matlab/Simulink, the Bode plot characteristics can be derived for different values of inertia constant and damping as shown in Fig. 4 and Fig. 5. It can be easily observed that inertia constant H has an impact primarily on the slope hight of the magnitude characteristic at low frequencies (denoted as R_H) and the horizontal position (natural frequency ω_n) of the peak response, while the damping coefficient D impacts mainly on the sharpness and vertical position (amplitude) of the peak response. Those observed features can, therefore, be used to estimate values of H and D from an experimentally captured Bode plot.

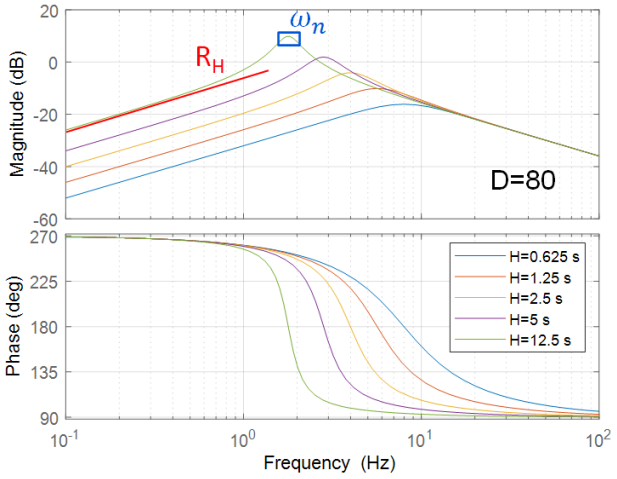

Fig. 4. Impact of inertia constant on the Bode characteristic

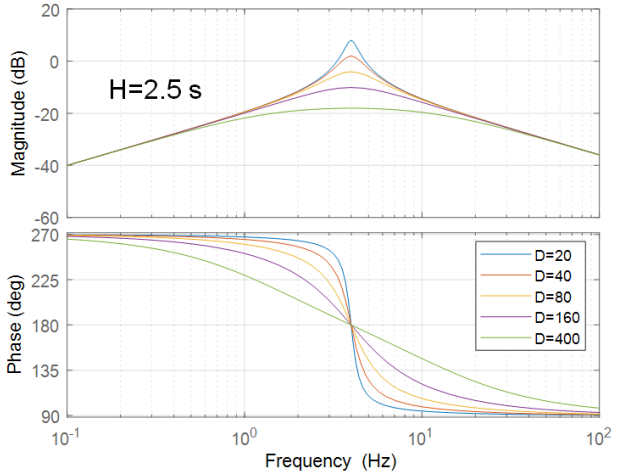

Fig. 5. Impact of damping factor on the Bode characteristic

First, looking at the inertia constant H, its value can be derived from the known expression describing the asymptote R_H as shown equation (11). By choosing a single point i (or an average of several points to achieve higher accuracy) on a linear part of the amplitude characteristic we can obtain $R_{H(i)}$ and $f_{NFPmod(i)}$ and thus calculate H by rearranging (11).

$$R_H = 2H\left(\frac{f_{NFPmod}}{f_0}\right) \tag{11}$$

Alternatively, it is also possible to obtain H from the known (i.e. assessed from the plot) value of the natural frequency ω_n, and the expression for this frequency (12) which depends on the inertia constant H. Again, with all other parameters being known, the value of H can be established by rearranging (12).

$$\omega_n = \sqrt{\frac{K_x\,\omega_0}{2H}} \tag{12}$$

In order to obtain a damping factor D the shape around the amplitude peak response can be used. As described in [17] three frequencies need to be found, one corresponding to the peak response (f_n), and the other two (f_1 and f_2), one on either side of f_n, with amplitude 3dB below the peak, as shown in Fig. 6. With those three frequencies the value of the damping quality factor Q can be calculated as:

$$Q = \frac{f_n}{f_2 - f_1} \tag{13}$$

Knowing that the damping ratio ζ is related to the damping quality factor as $\zeta = \frac{1}{2Q}$, and at the same time the damping ratio can be expressed as:

$$\zeta = \frac{D}{4}\sqrt{\frac{2X_{GFC}}{H\omega_0}} \tag{14}$$

where X_{GFC} is the per-unit reactance between the system voltage and the generator (or converter) internal voltage, the value of D can be derived from equation (14).

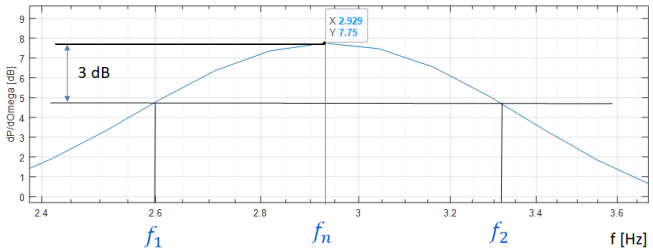

Fig. 6. Establishing the damping quality factor from the Bode plot

Additionally, both parameters H and D can be obtained through curve fitting of the measured amplitude characteristic points into the known amplitude response equation (15) obtained from the transfer function representing the generator swing equation (refer to Fig. 2).

$$|R|(\omega) = \left|\frac{K_x \cdot j\omega}{(j\omega)^2 + \frac{D \cdot j\omega}{2H} + \frac{K_x\omega_0}{2H}}\right| \tag{15}$$

A curve fitting based example is presented in Fig. 7 where the dynamic simulation model of a synchronous machine was utilised to obtain the frequency characteristic which was subsequently fitted into the equation (15) in order to obtain the unknown values of H, D and K_x. It is worth noting that the curve fitting based method can deal with more

than two unknowns, as it was in this case. The assumed value of the machine inertia constant in this example was H=5.2s and the value obtained from the estimation was H_{est} = 5.56s.

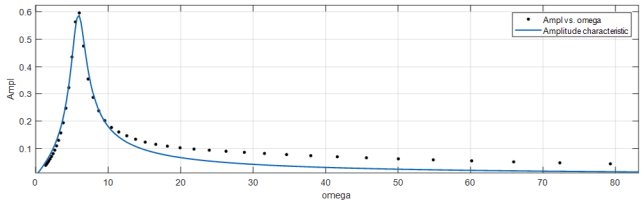

Fig. 7. Establishing H and D through amplitude characteristic curve fitting

Selected results of inertia parameter estimation using frequency-based methods applied to synchronous machine model are included in Table III.

Table III. Comparison of actual and estimated H using the frequency ramp method

Method	Measured parameter	Assumed value	Estimated value	Error
Low-frequency asymptote	H	5 s	4.85 s	3.0%
Peak-response	H D	5 s 40	4.64 s 41.96	7.2% 4.9%
Transfer function curve fitting	H D	5 s 40	4.68 s 36.84	6.4% 7.9%

C. Constant Frequency Ramp Tests

As illustrated in (2), for synchronous machines, when the grid frequency decreases with a constant rate, i.e. with a constant RoCoF, the SGs will release a near constant inertia power during steady state (assuming the frequency deviation is relatively small). Therefore, for grid forming converters emulating SG's inertial response, similar response is expected. Based on the block diagram shown in Fig. 2, the follow equations (16)-(18) could be derived:

$$\Delta\omega_{pu}^{GFC} = -\frac{\Delta P_{pu}}{2Hs} \tag{16}$$

$$\Delta\omega_{pu} = \Delta\omega_{pu}^{GFC} - \Delta\omega_{pu}^{grid} \tag{17}$$

$$\Delta P_{pu} = \Delta P_{pu}^{1} + \Delta P_{pu}^{2} = \frac{K_x\,\omega_0\,\Delta\omega_{pu}}{s} + D\Delta\omega_{pu}^{GFC} \tag{18}$$

which yield:

$$\frac{-\Delta P_{pu}}{\Delta\omega_{pu}^{grid}} = \frac{K_x\,\omega_0\,s}{s^2 + \frac{D}{2H}s + \frac{K_x\omega_0}{2H}} \tag{19}$$

Therefore,

$$\Delta P_{pu} = \frac{K_x\omega_0 s\Delta\omega_{pu}^{grid}}{s^2 + \frac{D}{2H}s + \frac{K_x\omega_0}{2H}} = \frac{-K_x\,\omega_0\,\dot{\Delta\omega}_{pu}^{grid}}{s^2 + \frac{D}{2H}s + \frac{K_x\omega_0}{2H}} \tag{20}$$

In the per-unit system, $\dot{\Delta\omega}_{pu}^{grid} = RoCoF_{pu}$, therefore:

$$\Delta P_{pu} = \frac{-2H}{\frac{2H}{K_x\omega_0}s^2 + \frac{D}{K_x\omega_0}s + 1} \times RoCoF_{pu} \tag{21}$$

During steady state,

$$\Delta P_{pu} = \lim_{s\to 0}\left(\frac{-2H}{\frac{2H}{K_x\omega_0}s^2 + \frac{D}{K_x\omega_0}s + 1} \times RoCoF_{pu}\right) \tag{22}$$

$$= -2H \times RoCoF_{pu}$$

thus, the inertia constant can be calculated by the measured ΔP_{pu} as shown in (23).

$$H = \frac{-\Delta P_{pu}}{2 \times RoCoF_{pu}} \tag{23}$$

In this method, the damping factor could not be estimated directly. Therefore, if damping factor is required, then the time or frequency domain methods can be used as discussed in previous sections.

Fig. 8 shows the results from simulating an analytical model shown in Fig. 2 with D = 40, a frequency ramp of 0.2 Hz/s, and H = 2, 4 and 6 respectively. From the measured ΔP_{pu} shown in Fig. 8 and using (23) the values of can be calculated as 2, 4, and 6, which align well with the previous analysis.

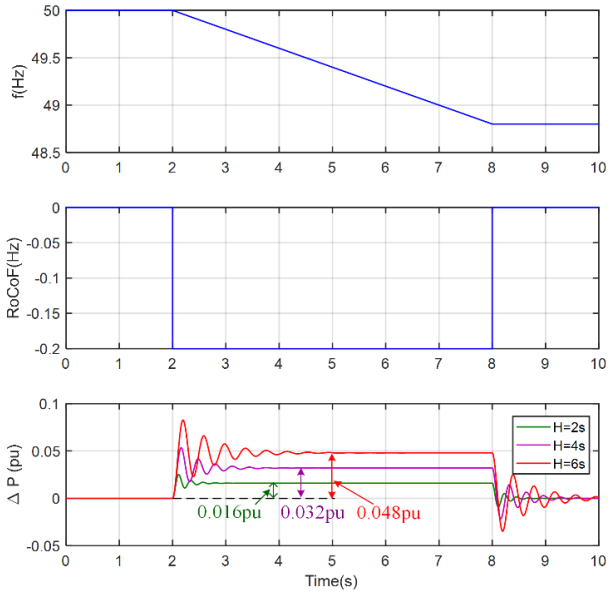

Fig. 8. Simulation of analytical model with different configured H.

To further validate the frequency ramp testing method, simulation is also conducted in a test network model with detailed SG and GFC models as illustrated in Fig. 9. In this test network, a SG model and a battery-GFC system model are both connected to a controllable voltage source, which is used to emulate the grid. The frequency ramp is achieved by controlling the controllable voltage source, and the SG and GFC were tested separately via the use of the switches shown. The test results are shown in Fig. 10. In the tests, a frequency ramp of 0.2 Hz/s (i.e. 0.004 pu/s) was applied from t = 5 s for 10 s. The power response from the SG and the GFC are shown in last two plots in Fig. 10, which can be used for calculating H via (23). The rating of the SG and GFC are both 246 kVA. The comparison of the estimated and actual values for H (i.e. H_{est} and H_{act}) are presented in Table IV.

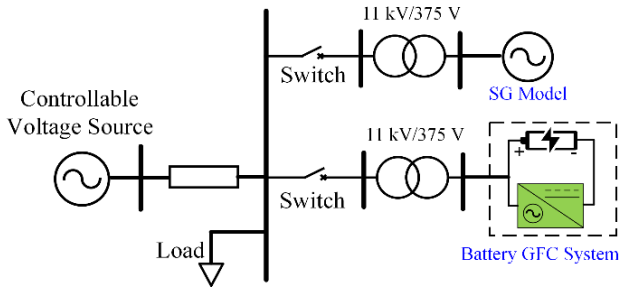

Fig. 9. Test network for frequency ramp tests

Table IV. Comparison of actual and estimated H using the frequency ramp method

Case	Device	$RoCoF_{pu}$	ΔP_{pu}	H_{est}	H_{act}	Error
1	SG	-0.004pu/s	0.0158 pu	1.975 s	2 s	1.25%
2	GFC		0.0324 pu	4.05 s	2 s	102.5%
3	GFC		0.0478 pu	5.975 s	4 s	49.25%

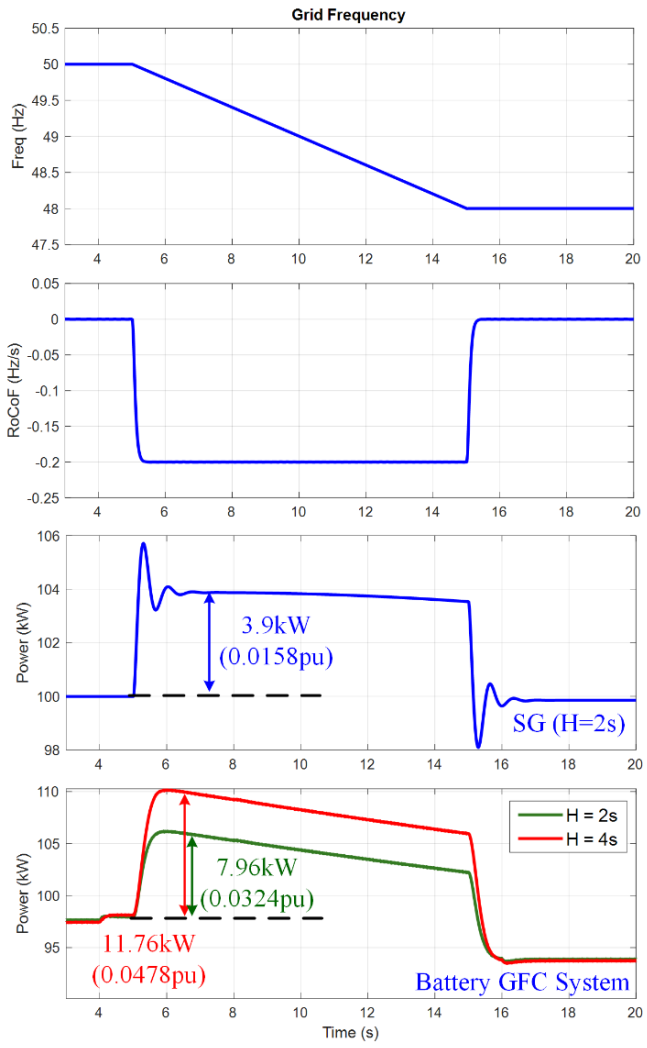

Fig. 10. Simulation of detailed SG and GFC models

It can be seen that when applying the method for the SG model, the result aligns very well with the actual configured H value with only an error of only 1.25%. However, in the tests for the GFC unit, the errors are relatively large. This could be due to the following reasons:

- The rated apparent power base that is actually used in the control loop is different from the claimed capacity of the GFC unit. This could typically be resolved by checking with the manufacturer who supplies the model and GFC system. In this case, the base power has been checked with the model supplier, confirming the consistency of the base power used.
- The controller of the GFC has additional control loops that lead to the behaviour of the system being different from the analytical model presented in Fig. 2. In this particular case, it is considered that there is a slower outer control loop being implemented which leads to the slow decrease of the power over time. Furthermore, there could also be other built-in mechanism in the controller to intentionally overdamp the GFC to ensure stability. This raises the question whether the flexible implementation of the GFC could lead to difficulties in the testing, and it is important to have a high level knowledge of the controllers to determine whether a test method is suitable or not. Those issues need to be further explored in detail in relevant expert workgroups and standardisation committees.

V. Discussion and Comparative Analysis of Inertial Response Testing

There are several ways inertial response could be measured on a physical GFC, depending on the converter rating, availability of testing equipment, and the purpose of the test (factory/prototype testing or network operation commissioning). All such tests can be generally classified into two groups.

Firstly, a controlled voltage source can be utilised, with sufficient power so that the device under test (DUT) does not influence the applied voltage waveform. This is believed to be the most reliable and definitive test as it captures a response to the actual disturbance but is limited by the power and availability of the dedicated test equipment.

Secondly, a low power control signal input can be utilised within the converter (if available) to provide the required disturbance mimicking the actual system event, while the terminal voltage of the converter is kept constant. This is only possible if the required disturbance signal is made accessible within the controller by the manufacturer. One alternative to this solution would be that instead of providing a signal input (which could be seen as risky by some manufacturers), the converter firmware could perform the whole test procedure such as NFP internally using an internally generated sinusoidal signal. In fact, such features are already available on some modern designs but currently only accessible for development purposes – the process is still quite manual to operate on site, and to perform the data analysis. When it comes to voltage phase jumps, applying an internal step to the bridge phase angle is relatively straightforward, and the resulting interaction with the system is more-or-less the same as if a real phase step happened at the grid. The same method can also be used to “inject” fake RoCoF ramps in a similar way, using a parabolic phase trajectory instead of a step.

Table V. Comparison of Methods for Evaluating the inertia response from GFCs

Method type	Advantages	Limitations
Time domain method	• Angle and/or power step can be performed more easy • The result (both *H* and *D*) can be obtained from a single test	• Vulnerable to measurement noise • Less accurate compared to frequency based methods
Frequency based method	• High accuracy and robust against measurement noise • Can identify adverse control interactions as the whole frequency spectrum is obtained	• Grid voltage emulator (or amplifier) is required, which can be difficult for large GFC systems • Number of tests required is much higher compared to the other two methods.
Frequency ramp method	• For GFCs system that has close to a SG's inertial behavior, relatively high accuracy can be achieved. • Easy to implement the test, where only a frequency ramp is required to apply on the GFC.	• Similar to the frequency-based method, a grid emulator is required, which can be difficult for large GFC systems • It is difficult (if not impossible) to assess damping coefficient

Finally, the safest (but perhaps not fully reliable) method would be to test the controller response only by coupling it with a real-time simulator such as RTDS.

The methods based on converter control signal perturbation (e.g. PWM reference voltage phase angle) are suitable for any generator size and can, therefore, be used for the purposes of large power park commissioning tests, which power grid providing a fixed voltage source. It should be also noted that the frequency-based analytical methods are only suitable for characterising linear systems, or the systems which can be assumed linear in the vicinity of the steady state operating point. Therefore, when deriving the frequency characteristic empirically it is important to bear in mind the maxim allowable power oscillation amplitude. To do so, the magnitude of the input signal modulation needs to be carefully controlled, especially as the modulation frequency increases. Typically, the active power modulations should be kept below 1-3% of rated power, otherwise some concerns may arise about vibrations coupling through to mechanical systems (e.g. in a wind-park), especially at certain modulation frequencies.

Based on the such practical consideration and taking into account the indicative parameter estimation accuracy as presented in this paper, Table V includes a comparative analysis of different testing methods with their strengths and perceived limitations.

VI. Conclusions

Three different groups of methods to assess the inertia and damping performance of grid forming converter controllers have been presented. All presented methods are based on the synchronous machine swing equation. The time domain, frequency domain and frequency ramp methods have shown a potentially good accuracy in estimating the inertia and damping time constants. The selection of the methods will depend on the availability of equipment or internal signals to perform the test, specific characteristics of the converter controller, as well as its size.

More detailed analysis and the development of standard testing guidelines are needed, in order to facilitate rapid and safe adoption of the GFCs which offer software-based implementation of inertial behaviour.

Acknowledgement

The authors would like to thank all partners involved in the Battery-VSM project funded by National Grid ESO in the UK, and the VerbundnetzStabil project financed by the German Federal Ministry of Economic Affairs and Energy BMWi for providing support as well as lively discussions on the topic. A short summaries of those two projects are included below:

The Battery-VSM (Virtual Synchronous Machine) project, funded by National Grid ESO in the UK and partners Belectric GmbH, University of Strathclyde and GE Renewable Energy, aims to test and demonstrate the capability and performance of a 246 kVA inverter-interfaced battery-powered VSM system under a highly realistic 11 kV / 400 V physical network environment. The project will evaluate the capability of VSM under a wide range of network operating conditions, such as inertial response during frequency disturbances, reactive power support during voltage disturbances, dynamic behaviour during system faults, performance during grid connected and islanded mode, and capability of black starting as an island.

VerbundnetzStabil is a project financed by the German Federal Ministry of Economic Affairs and Energy BMWi (FKZ 0350015) with the partners KACO new energy GmbH, TransnetBW GmbH, University of Stuttgart (IFK) and Fraunhofer ISE. It investigates the stability of converter dominated transmission and distribution networks. The focus of this project is on grid events in which the inverter reaches its current limit. With the resulting requirements, a new controller is developed to meet the criteria. The basic control structure will be used for large transmission grid simulations in order to investigate the stability. As a final step a real test will be carried out in the MW-Lab at Fraunhofer ISE.

VII. References

[1] B. Kroposki et al., "Achieving a 100% Renewable Grid: Operating Electric Power Systems with Extremely High Levels of Variable Renewable Energy", IEEE Power and Energy Magazine, vol. 15, no. 2, pp. 61–73, Mar. 2017, DOI: 10.1109/MPE.2016.2637122.

[2] A. Tayyebi, F. Dorfler and F. Kupzog, "Grid Forming Converters - Inevitability, Control Strategies and Challenges in Future Grid Application", June 2018, available online: https://www.cired-repository.org/handle/20.500.12455/1249.

[3] ENTSO-E, “High Penetration of Power Electronic Interfaced Power Sources (HPoPEIPS) - ENTSO-E Guidance document for national implementation for network codes on grid connection”, Mar. 2017, available online: https://consultations.entsoe.eu/system-development/entso-e-connection-codes-implementation-guidance-d-3/user_uploads/igd-high-penetration-of-power-electronic-interfaced-power-sources.pdf.

[4] ENTSO-E, “Technical Report: High Penetration of Power Electronic Interfaced Power Sources and the Potential Contribution of Grid forming Converters”, Jan. 2020, available online: https://www.entsoe.eu/events/2020/01/30/workshop-on-high-penetration-of-power-electronic-interfaced-power-sources-and-the-potential-contribution-of-grid-forming-converters/.

[5] MIGRATE Project, “Deliverable 3.1: Description of System Needs and Test Cases”, Jan. 2020, available online: https://www.h2020-migrate.eu/downloads.html.

[6] MIGRATE Project, “Deliverable 3.6: Requirement guidelines for operating a grid with 100% power electronic devices”, Jan. 2020, available online: https://www.h2020-migrate.eu/downloads.html.

[7] WindEurope position paper, “Future system needs and the role of grid-forming converters”, July 2019, available online: https://windeurope.org/policy/position-papers/future-system-needs-and-role-of-grid-forming-converters.

[8] M. Baller, National grid ESO, “Draft Grid Code – Grid Forming Converter Specification 3rd September 2020”, 2020.

[9] VDE FNN Netztechnik/Netzbetrieb, “FNN Guideline: Grid forming behaviour of HVDC systems and DC-connected PPMs”, 2020.

[10] National Grid ESO, “Stability Pathfinder Phase Two: Technical Performance Requirements,” Sept. 2020, available online: https://www.nationalgrideso.com/research-publications/network-options-assessment-noa/network-development-roadmap [accessed on 12th Oct. 2020

[11] National Grid ESO, “Draft Grid Code – Grid Forming Converter Specification 3rd September 2020”, Sept. 2020, available online: https://www.nationalgrideso.com/industry-information/codes/grid-code-old/modifications/gc0137-minimum-specification-required [accessed on 12th Oct. 2020]

[12] ENTSO-E, “Technical Report: High Penetration of Power Electronic Interfaced Power Sources and the Potential Contribution of Grid forming Converters,” Jan. 2020, available online: https://www.entsoe.eu/events/2020/01/30/workshop-on-high-penetration-of-power-electronic-interfaced-power-sources-and-the-potential-contribution-of-grid-forming-converters/ [accessed on 12th Oct. 2020]

[13] D'Arco, S., & Suul, J. A. (2015, June). A synchronization controller for grid reconnection of islanded virtual synchronous machines. In 2015 IEEE 6th International Symposium on Power Electronics for Distributed Generation Systems (PEDG) (pp. 1-8). IEEE.

[14] D’Arco, S., Suul, J. A., & Fosso, O. B. (2015). A Virtual Synchronous Machine implementation for distributed control of power converters in SmartGrids. Electric Power Systems Research, 122, 180-197.

[15] Zhong, Q. C., & Weiss, G. (2010). Synchronverters: Inverters that mimic synchronous generators. IEEE Transactions on industrial electronics, 58(4), 1259-1267.

[16] M. Yu et al., “Instantaneous penetration level limits of non-synchronous devices in the British power system”, IET Renewable Power Generation, vol. 11, no. 8, pp. 1211–1217, 2017, doi: 10.1049/iet-rpg.2016.0352.

[17] “How to calculate damping from a FRF?”, https://community.sw.siemens.com/s/article/how-to-calculate-damping-from-a-frf [accessed on 30th Oct. 2020]